

Simulated Tempering-Enhanced Umbrella Sampling Improves Convergence of Free Energy Calculations of Drug Membrane Permeation

Carla F. Sousa, Robert A. Becker, Claus-Michael Lehr, Olga V. Kalinina, and Jochen S. Hub*



Cite This: *J. Chem. Theory Comput.* 2023, 19, 1898–1907



Read Online

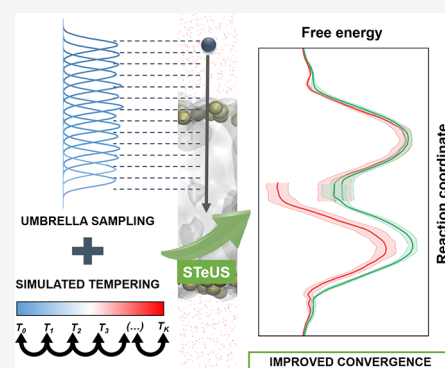
ACCESS |

Metrics & More

Article Recommendations

Supporting Information

ABSTRACT: Molecular dynamics simulations have been widely used to study solute permeation across biological membranes. The potential of mean force (PMF) for solute permeation is typically computed using enhanced sampling techniques such as umbrella sampling (US). For bulky drug-like permeants, however, obtaining converged PMFs remains challenging and often requires long simulation times, resulting in an unacceptable computational cost. Here, we augmented US with simulated tempering (ST), an extended-ensemble technique that consists in varying the temperature of the system along a pre-defined temperature ladder. Simulated tempering-enhanced US (STeUS) was employed to improve the convergence of PMF calculations for the permeation of methanol and three common drug molecules. To obtain sufficient sampling of the umbrella histograms, which were computed only from the ground temperature, we modified the simulation time fraction spent at the ground temperature between $1/K$ and 50%, where K is the number of ST temperature states. We found that STeUS accelerates convergence, when compared to standard US, and that the benefit of STeUS is system-dependent. For bulky molecules, for which standard US poorly converged, the application of ST was highly successful, leading to a more than fivefold accelerated convergence of the PMFs. For the small methanol solute, for which conventional US converges moderately, the application of ST is only beneficial if 50% of the STeUS simulation time is spent at the ground temperature. This study establishes STeUS as an efficient and simple method for PMF calculations, thereby strongly reducing the computational cost of routine high-throughput studies of drug permeability.



INTRODUCTION

Molecular dynamics (MD) simulations are a powerful computational tool used to obtain an atomistic view of biological processes.¹ Nevertheless, studying complex biological systems using MD simulations remains challenging since it requires obtaining exhaustive sampling of the high-dimensional configurational space, which is time-consuming owing to slow conformational dynamics and long autocorrelation times. For instance, simulating systems that include biological membranes at atomic details is challenged by the sticky environment of the head group regions, leading to slow rearrangements of biomolecules or other solutes and, thereby, to slow conformational sampling.^{2–5}

Fast and faithful simulation of such systems is, however, very valuable, since solute permeation across biomembranes is highly relevant in the field of drug discovery. Most drugs need to pass multiple cellular membranes to reach their targets such as the intestinal barrier or the blood–brain barrier.⁶ Certain antibacterial drugs, specifically, need to pass one or even two bacterial membranes to reach their target.⁷ The potential of mean force (PMF, alternatively called the free energy profile) for solute translocation across the membrane can be calculated from MD simulations, providing a spatially resolved view on

solute partitioning between water and membrane.^{4,8–10} Solute permeability is typically calculated from the PMF together with the position-dependent diffusion coefficient by using the inhomogeneous solubility-diffusion model.^{8,9,11–14} In this study, we focus on the PMFs because variations of solute permeabilities are mostly determined by variations of the PMF.

For most solutes, membrane permeation is a rare event. Calculating membrane permeability from unbiased simulations with the counting method is theoretically possible but would still require large simulation times for most permeants.¹⁵ Hence, enhanced sampling methods are crucial for computing the PMF ($G(z)$)^{16,17} such as path sampling,¹⁸ adaptive biasing force,¹⁹ metadynamics,^{20,21} or umbrella sampling (US).²² US is among the most widely used enhanced sampling techniques for computing PMFs and will be used in this study. It involves the division of the process in windows along a preselected reaction

Received: November 17, 2022

Published: February 28, 2023



coordinate (RC), while the application of restraining potentials ensures sampling of unfavorable regions of high free energy.^{22–26} These US windows must overlap to sample the complete RC. The PMF is typically obtained by unbiasing the probability distributions from the restrained simulations, using the weighted histogram analysis method (WHAM).²⁷ An alternative to WHAM is the dynamic histogram analysis method that, in addition to probabilities along the RC, also makes use of dynamic information on transitions between bins along the RC.²⁸

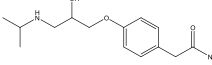
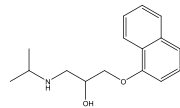
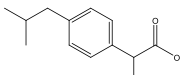
For simulations of solute translocation across lipid bilayers, the relative center of mass displacement between solute and membrane along the membrane normal (z coordinate) has been often used as RC, thereby sampling the complete permeation event.^{20,25,29,30} However, such protocol does not accelerate the convergence of orthogonal degrees of freedom such as the solute orientation, solute–lipid interaction patterns, or the lipid–lipid arrangements. Specifically, simulations of solute insertion in lipid bilayers were found to be affected by the slow reorganization of the ionic interactions between the phospholipid headgroups and the solute.^{2,5,31} Slow sampling of such orthogonal degrees of freedom may lead to a poor convergence in standard US simulations. Although such problems can in principle be overcome using multi-dimensional US along a set of RCs, finding good RCs is difficult in practice, good RCs may be solute-dependent, and multi-dimensional US is computationally expensive.³²

Sampling challenges have been addressed by extended-ensemble methods that, in contrast to conventional US, do not require the definition of RCs.^{33–38} One possibility is to use generalized ensemble algorithms in temperature space, such as the simulated tempering (ST) method.^{39,40} ST aims to achieve broader sampling by periodically changing the temperature during the simulation along a pre-defined temperature ladder. During ST simulations, increased temperatures help the system to overcome enthalpic barriers and, thereby, to enhance the conformational sampling. Importantly, unlike simulated annealing that drives the system out of equilibrium, ST maintains equilibrium and produces well-defined thermodynamic ensembles. Hybrid methods that combine RC-based with extended ensemble-based methods have also been proposed.^{14,41–44}

In this study, we introduce a new protocol for combining ST with US (ST-enhanced US, or STeUS) and analyze its benefit for calculating PMFs for solute permeation, by comparing the convergence of the PMFs between standard US and STeUS. To cover solutes of different molecular weights, area/volume, and polarity, we simulated the permeation of methanol, ibuprofen, 1-propranolol, and atenolol (Table 1). Except for methanol, these molecules are widely used drugs with common physicochemical properties, suggesting that our results are representative for future simulations in drug development. We show that STeUS is a promising approach for improving the efficiency and accuracy of free energy calculations of membrane permeation.

In ST, weights are applied to control the occupancies of the K temperature states ($T_0 \dots T_{K-1}$), while these weights are often optimized to obtain uniform occupancies among the temperature states. For US, however, uniform occupancies may not be optimal, because only a fraction of $1/K$ of the simulation time is available for collecting the umbrella histograms at the physiologically relevant ground temperature T_0 . Therefore, we devised a modified simulated tempering-

Table 1. Physicochemical Properties of the Molecules Used in this Study

molecule	MW (g/mol)	VdW volume (Å ³) ^a	min. projection area (Å ²) ^a	max. projection area (Å ²) ^a	$c \log K_p$
methanol 	32.04	36.8	11.18	15.32	-0.52
atenolol 	266.34	261.3	36.85	87.58	0.42
1-propranolol 	259.35	257.6	41.97	85.55	2.58
ibuprofen 	206.28	211.8	35.44	64.57	3.84

^aProperties calculated using the Chemicalize platform, <https://chemicalize.com/>, developed by Chemaxon [May 2022]. $c \log K_p$, predicted octanol–water partition coefficient.

enhanced US (STeUS) protocol that allows an increased, user-defined occupancy P_0 of the ground temperature T_0 , while all higher temperature states remain uniformly populated. In the Results section, we show that the benefit of using an increased occupancy of the ground temperature depends on the solute's physicochemical characteristics, especially its size. We found that for small molecules such as methanol, the simulation time spent at T_0 might limit the convergence of the umbrella histograms, suggesting the use of higher values of P_0 . For bulkier, drug-like solutes, in contrast, longer simulation times at higher temperatures were most critical for convergence, suggesting that only a moderately increased P_0 is most beneficial for obtaining rapid sampling.

THEORY

Simulated Tempering. In ST, the temperature is a dynamic variable, and a random walk is performed on the temperature ladder of ($T_0 \dots T_{K-1}$).^{39,45} The appropriate choice of the temperature ladder is important: T_0 typically corresponds to the physiologically relevant temperature while T_{K-1} should be high enough to aid the transition over relevant free energy barriers.

Let x denote the configuration and $n = 0, \dots, K - 1$ the temperature state, and then the probability distribution $P(x, n)$ is

$$P(x, n) \propto e^{-H(x, n)} \quad (1)$$

where the generalized Hamiltonian $H(x, n)$ is defined by

$$H(x, n) = \beta_n H(x) - g_n \quad (2)$$

with $\beta_n = 1/k_B T_n$ being the inverse temperature and g_n the weight for the n th temperature. Hence, the partition function is

$$Z = \sum_n \int dx e^{-H(x, n)} = \sum_n Z_n e^{g_n} \quad (3)$$

where Z_n is the partition function for state n with temperature T_n . The Hamiltonian implies a generalized ensemble with canonical ensembles for each temperature, while relative weights of the temperatures are modified with the parameters g_n .

Typical ST simulations involve common MD simulations at a constant temperature T_n with updates to neighboring temperatures T_{n+1} or T_{n-1} . Transitions between T_n and $T_{n\pm 1}$ are performed according to the Metropolis criterion with a probability⁴⁶

$$w(T_n \rightarrow T_{n\pm 1}) = \min(1, e^{-((\beta_{n\pm 1} - \beta_n)H(x) - (g_{n\pm 1} - g_n))}) \quad (4)$$

thereby maintaining detailed balance and well-defined canonical ensembles. During a burn-in phase at the beginning of the simulation, the weights g_n are typically optimized to obtain uniform occupancies of all temperature states.

The burn-in phase is greatly accelerated by choosing good initial weights, as suggested by Park and Pande.⁴⁷ Accordingly, requesting that optimal weights yield equal acceptance for transition $T_n \rightarrow T_{n+1}$ and $T_{n+1} \rightarrow T_n$ we have $\Delta H_{n \rightarrow n+1} = \Delta H_{n+1 \rightarrow n}$ with

$$\Delta H_{n \rightarrow n+1} \approx (\beta_{n+1} - \beta_n)E_n - (g_{n+1} - g_n)$$

and

$$\Delta H_{n+1 \rightarrow n} \approx (\beta_n - \beta_{n+1})E_{n+1} - (g_n - g_{n+1}) \quad (5)$$

Hence, the relative weights can be calculated from

$$g_{n+1} - g_n \approx (\beta_{n+1} - \beta_n) \frac{E_n + E_{n+1}}{2} \quad (6)$$

where E_n is the average potential energy of the system at T_n , which can be taken from a short simulation.

Increased Occupancy of the Ground Temperature. In this study, the weights were updated with the Wang–Landau algorithm.⁴⁸ This approach involves updating the weights (g_n) by an incremental factor (δ) with the goal to obtain a uniform histogram over the temperature states. During a burn-in phase, the weights are optimized in rounds, where each round involves a random walk over the temperature states using a given set of initial g_n . In every state transition, g_n is updated by $g_{n,\text{new}} = g_{n,\text{old}} \times \delta$, until a flat histogram over temperature is achieved, indicating the convergence of g_n with an accuracy proportional to $\ln(\delta)$. In the next round, δ is reduced and a new random walk over the states is started. As the simulation proceeds, these steps are repeated, while δ decreases monotonically to 1, leading to an increasingly accurate convergence of g_n .⁴⁸

Whereas the traditional ST approach results in uniform occupancy over temperatures ($T_0 \dots T_{K-1}$), only the samples generated at the ground temperature (T_0) are typically physiologically relevant.⁴⁹ This is true for the specific case of PMF calculations for drug membrane permeation: while sampling at higher energies is essential to overcoming free energy barriers, only a small fraction of $1/K$ of samples at the ground temperature are correctly distributed to allow the construction of the PMF for the physiologically relevant temperature.

To accelerate the convergence of the umbrella histograms at T_0 , we devised a modified ST approach that spends an increased, user-defined, occupancy P_0 (instead of $1/K$) at the ground temperature. This was implemented with a reduced Wang–Landau incremental factor δ_{P_0} applied for the ground

temperature. Specifically, let P_h denote the occupancy of the higher states, and then we have $P_0 + (K - 1)P_h = 1$. Hence, δ_{P_0} was reduced by a factor of P_h/P_0 for the ground temperature, while the incremental for other states was chosen following the usual Wang–Landau method. A modified source code file `expanded.cpp` for GROMACS 2021 that implements the method is available as a [Supporting Information](#).

METHODS

The membrane system, comprising 32 palmitoyl-oleoyl-phosphatidylcholine (POPC) phospholipids and 50 water molecules per lipid in a cubic simulation box, was taken from Nitschke et al.³² Lipids were described using the modified Berger force field, as used by Nitschke et al.^{32,50,51} and water by the SPC model.⁵² Methanol was modeled using the Gromos43A1 force field, and the distance between the carbon and the hydroxyl hydrogen was constrained to allow the use of a 5 fs time step. Ibuprofen, atenolol, and 1-propranolol were modeled using the Gromos54A7 force field, with parameters from the Automated Topology Builder (ATB) website.⁵³ Since this study focuses purely on sampling, we did not further validate the force fields against experimental data.

MD simulations were performed and analyzed using GROMACS 2021^{54,55} and visualized using VMD.⁵⁶ The center of mass (COM) motion of the bilayer relative to the solvent was removed every 10 integration steps. COM groups were (i) each lipid monolayer and (ii) solvent and ligands. The particle-mesh Ewald (PME) method^{57,58} was used for long-range electrostatic interactions, with a real space cutoff of 1.2 nm and a Fourier spacing of 0.14 nm, and a 1.2 nm cutoff was used for the van der Waals interactions. Long-range dispersion corrections to pressure and energy were applied.⁵⁹ The velocity-rescale thermostat,⁶⁰ with 0.5 ps coupling constant, was used for temperature coupling and the Berendsen barostat,⁶¹ with 10 ps coupling constant, for pressure coupling. The LINCS algorithm was used to constrain all bonds of lipids and solutes.⁶² Water molecules were constrained with SETTLE.⁶³

Drugs were inserted into the system, as previously described:²⁵ two drugs molecules were inserted into the system (one into water, $z = -3.5$ nm, and the other at the bilayer center, $z = -0.2$ nm) by gradually switching on their van der Waals and Coulombic interactions with the system, using 10 λ steps (0.6 ns each). The COM position of the solute relative to the bilayer along the bilayer normal (z) was used as the RC for US simulations.²² Here, only lipid atoms within a cylinder of radius 1.5 nm around the solute were used to compute the bilayer COM, as implemented in the pull geometry “cylinder” of the GROMACS code. Initial structures for each of the 37 US windows were generated using sequential 5 ns simulation, where the solutes were pulled over a distance of $\Delta z = 0.1$ nm in each simulation. Each US window was simulated for 100 ns, using a harmonic force constant of 1000 $\text{kJ}\cdot\text{mol}^{-1}\cdot\text{nm}^{-2}$, and the productions were repeated five times. The first 10 ns were removed for equilibration, and PMFs were constructed using WHAM.^{27,64} Five replications were performed for each system tested in this study. Errors of the profiles for each individual replica were estimated using the Bayesian bootstrap analysis of complete histograms, using a total of 200 bootstraps.⁶⁴ Errors of the profiles for the average of the five replicas represent the standard deviation between these data.

For the simulated-tempering protocol, the md velocity Verlet (md-vv) integrator was used. Nine temperatures were used ($T_0 = 300$ K ... $T_8 = 348$ K) with a $\Delta T = 6$ K. Initial weights were determined as described by Park and Pande.⁴⁷ Sequential short simulations (10 ps) were performed for each temperature (T_0 ... T_8), and the weights were determined from the average potential energy, at each temperature. A change of temperature was attempted every 500 integration steps and accepted or rejected according to the Metropolis criterion. The temperature of the system along the simulation time revealed frequent swapping between the temperatures, showing that the temperatures were well mixed in the STeUS simulations (Figure S1).

Three values of target occupancy of the ground temperature (P_0) were tested: according to the standard ST protocol, $P_0 = 1/9$, and, according to the modified ST protocol, $P_0 = 0.2$ or $P_0 = 0.5$ (Figure 1).

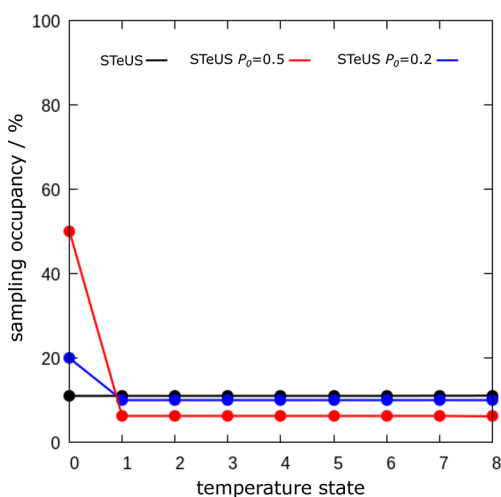


Figure 1. Occupancy of temperature states ($T_0 = 300$ K, ..., $T_8 = 348$ K; $\Delta T = 6$ K) in simulations with ibuprofen for STeUS with uniform occupancies (black) or with increased occupancies of $P_0 = 0.2$ and $P_0 = 0.5$ for the ground temperature (blue and red, respectively).

RESULTS

Standard US Leads to Poor Convergence of PMFs for Drug-Like Permeants. PMFs of solute translocation across the POPC bilayer were obtained with traditional US, comprising a 100 ns simulation time per window, while omitting 10 ns for equilibration, each window being simulated five times (Figure 2 and Figure S2). PMFs were computed for solute translocation from bulk water into the membrane center (inward direction) and from the membrane center to bulk water (outward direction). Because the bilayer is symmetric, converged PMFs of the two molecules should likewise be symmetric. Hence, in this work we used the absolute difference between the PMFs for inward and outward directions as a measure for the convergence of the PMFs (Figure S3). Considerable free energy offsets between the PMF for the inward and outward directions are evident for all bulkier drug-like permeants—atenolol, 1-propranolol, and ibuprofen—indicating major hysteresis problems and poorly converged PMFs. This conclusion is also supported by a large difference between the PMFs of the five independent replicas (Figure S2 and Figure 2). At the same time, PMFs for the smaller

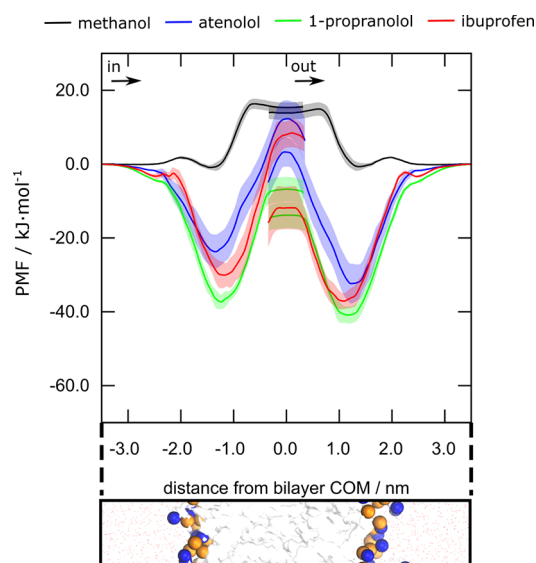


Figure 2. PMFs of membrane permeation using conventional US. PMFs are shown for methanol (black), atenolol (blue), 1-propranolol (green), and ibuprofen (red) as a function of distance to the bilayer COM at $z = 0$ nm, based on five independent replicas for each solute and 100 ns of simulation time. Shaded areas represent the standard deviation between the replicas. For reference, the lower panel shows the bilayer with water molecules depicted as red dots, membrane as a white surface, and phosphate and choline groups as orange and blue spheres, respectively.

permeant—methanol—show a by far better convergence and only minor hysteresis (Figure 2).

To test whether longer simulation times reduce the hysteresis error, we followed the PMFs using increasing simulation times of 20 to 100 ns in steps of 10 ns while consistently omitting the first 10 ns for equilibration (Figure 3). However, in this simulation time range, longer simulations reduced the hysteresis error only partly, suggesting that the hysteresis was caused by autocorrelations on longer time scales and that by far longer simulations would be needed to obtain converged PMFs with conventional US.

Statistical errors for each replica (Figure S2, shaded areas) were estimated by bootstrapping complete histograms. Such approach typically yields a conservative error estimate because it assumes that only different histograms are independent, but it does not assume a specific autocorrelation time within individual US windows. As evident from Figure S2, however, the statistical error dramatically underestimates the true error owing to hysteresis. This demonstrates that neighboring histograms are highly correlated and reinforces that the 100 ns of conventional US simulations were, by far, insufficient to obtain converged PMFs.

STeUS Accelerates the Convergence of PMFs.

Simulated tempering was integrated in the previous US protocol employing nine temperature states from 300 to 348 K in steps of $\Delta T = 6$ K, yielding a new STeUS protocol. Using it, the PMF at the ground temperature of 300 K was calculated (Figure 4 and Figure S4), equivalent to the temperature adopted during the conventional US simulations (Figure 2 and Figure S2).

The application of STeUS for the bulkier drug-like solutes atenolol, 1-propranolol, and ibuprofen led to a marked decrease in the offsets between the PMFs for the inward and outward directions (Figure 4 and Figure S4), demonstrating a

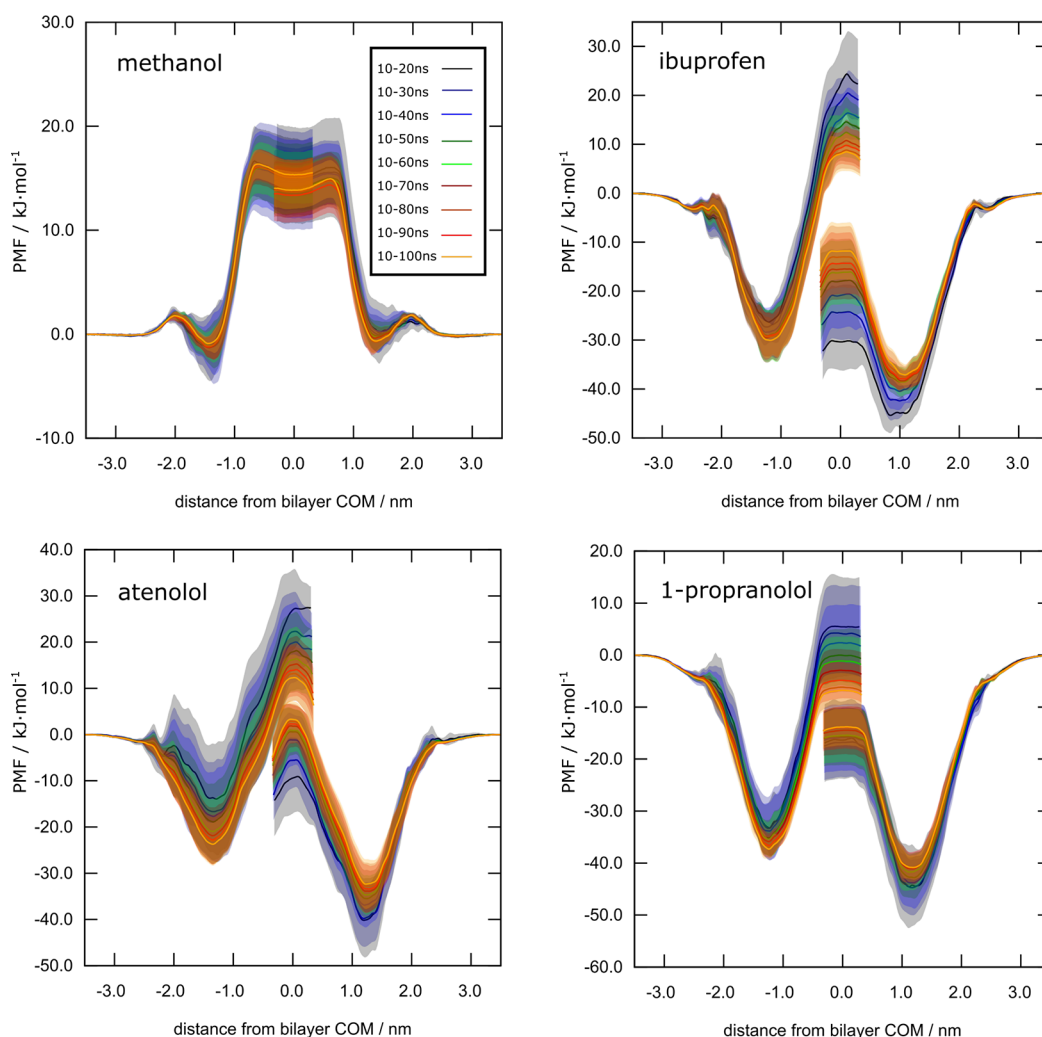


Figure 3. PMF from conventional US for methanol, ibuprofen, atenolol, and 1-propranolol, with increasing simulation times of 20 to 100 ns in steps of 10 ns. Shaded areas represent the standard deviation among five independent replicas.

significant decrease in hysteresis error for these solutes (Figure 5). In addition, the PMFs were more symmetric regarding the shapes and positions of the PMF maxima and minima, and the variability among the five independent replicas was considerably decreased, as compared to the standard US (Figure S4). These observations indicate greatly improved convergence of the PMFs within the time frame of the study with STeUS. Moreover, PMFs computed with increasing simulation times, in steps of 10 ns, from 20 to 100 ns indicate that, unlike US, the STeUS method yields reasonable convergence within short simulation times of 20 to 50 ns depending on the solute (Figure S5).

The impact of the improved convergence of the PMFs on the determination of macroscopic thermodynamic properties, which can be compared with experimental quantities, was assessed by calculating the partition coefficient ($\log K_p$) of the solutes to the model membrane after 30 and 100 ns of simulation times (Table S1). The application of the STeUS significantly reduced the error of $\log K_p$, with the error of the determination being already minimal after 30 ns of simulation and lower than the error of US after 100 ns. Further indication of faster convergence is the greatly reduced difference between the $\log K_p$ for the molecules in the inward and outward directions obtained with STeUS (Table S2).

STeUS Enhances Sampling for Bulky Permeants but Hardly for Methanol. The results reported above indicate that the enhanced convergence obtained by integrating ST in US is solute dependent. While the decrease in hysteresis error for the bulkier solutes was greater, for the small methanol STeUS only marginally reduced hysteresis (t -test, $p = 0.168$). Additional insights in the convergence is given by analyzing the average absolute difference between the PMFs for the molecules in the inward and outward directions as a function of simulation time, which gives a quantitative analysis of the hysteresis error (Figure 6). For all the bulkier permeants, atenolol, ibuprofen, and 1-propranolol, there is a substantial advantage in using STeUS relative to conventional US. With STeUS, the hysteresis after 20 ns is lower as compared to the hysteresis with conventional US after 100 ns, suggesting a more than five times accelerated convergence for the STeUS protocol (Figure 6B–D, black and green symbols). For methanol, however, the benefit of using STeUS is marginal and starts to be evident only after 60 ns of simulation (Figure 6A, black and green symbols). In fact, for methanol, the hysteresis error is very small for both US or STeUS, with the average absolute difference below $2 \text{ kJ}\cdot\text{mol}^{-1}$ after 30 ns of simulation. This can be explained by the small size of

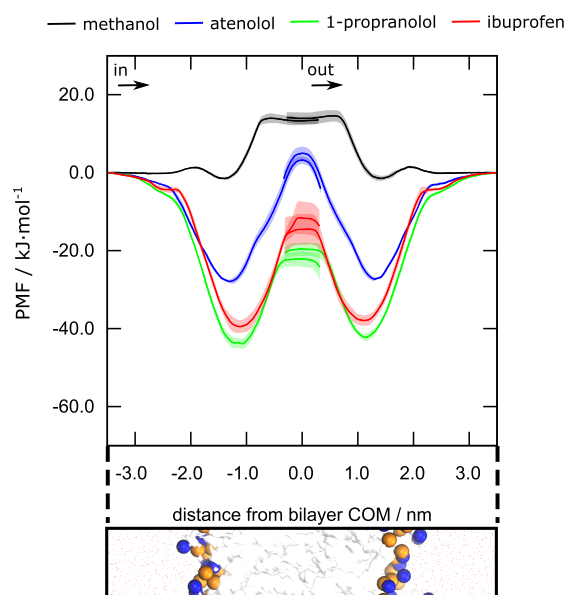


Figure 4. PMFs after 100 ns of simulation time using STeUS. PMFs for methanol (black), atenolol (blue), 1-propranolol (green), and ibuprofen (red) as a function of distance to the bilayer COM at $z = 0.0$ nm, based on five independent replicas for each solute. Shaded areas represent the standard deviation among the replicas. For reference, the lower panel shows the bilayer with water molecules depicted as red dots, membrane as a white surface, and phosphate and choline groups as orange and blue spheres, respectively.

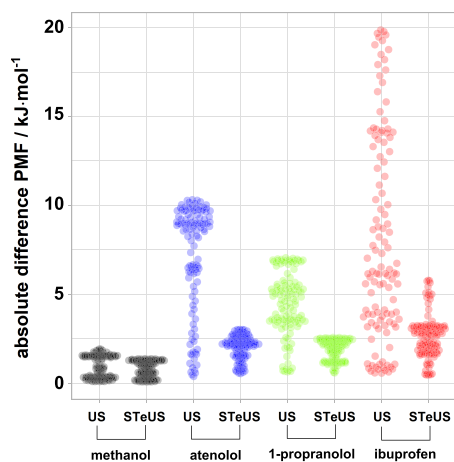


Figure 5. Absolute difference between the PMFs at symmetric pairs z -positions between $|z| = 2.5$ nm and $|z| = 0$ nm, collected from five independent PMFs based on conventional US (Figure 2) or STeUS (Figure 4); see labels along the abscissa. Each dot i refers to the absolute value of the free energy difference $|G(z_i) - G(-z_i)|$, where $z_i \in [0 \text{ nm}, 2.5 \text{ nm}]$ in steps of 0.1 nm, hence quantifying the hysteresis between the PMFs for inward and outward directions. Results are shown for (from left to right) methanol (black), atenolol (blue), 1-propranolol (green), and ibuprofen (red); see axis labels. STeUS greatly reduces the hysteresis relative to conventional US.

methanol, for which the convergence is much faster as compared to bulkier permeants.

Increasing the Occupancy of the Ground Temperature of STeUS Further Accelerates the Convergence of PMFs in a Solute-Dependent Manner. By applying STeUS, in which the system equally samples the different temperatures ($T_0 = 300$ K to $T_8 = 348$ K, $\Delta T = 6$ K), the time

spent at the ground temperature (300 K) is only approximately 11% of the total simulation time (Figure 1). Hence, since only the frames obtained from the simulation at 300 K were used to collect the umbrella histograms and, thereby, to compute the PMFs, errors also arose from insufficient simulation time at the ground temperature (Figure S5). These errors seem to affect especially the performance of STeUS, compared to US, for the smallest permeant methanol. To circumvent this problem, we implemented a modified ST protocol into GROMACS that allows defining the fraction P_0 of simulation time spent at the ground temperature (see Theory). As a control, applying the modified STeUS approach with $P_0 = 11\%$ yields similar results as standard STeUS because the occupancy of the ground state is similar (Figures S6 and S7).

Using the modified STeUS method, we computed PMFs either using $P_0 = 20\%$ or using $P_0 = 50\%$ (Figure 6, blue and red symbols, respectively). The rationale behind these choices was as follows: setting $P_0 = 50\%$ ensures extensive sample collection for the umbrella histograms at ground temperature at the cost of strongly reduced simulation time spent at high temperatures, thereby losing some conformational sampling relative to $P_0 = 11\%$; alternatively, setting $P_0 = 20\%$ approximately doubles the number of samples drawn at the ground temperature (relative to $P_0 = 11\%$ for standard STeUS), while focusing the majority of simulation time still toward high temperatures for improved conformational sampling. For methanol, $P_0 = 50\%$ leads to a slightly reduced hysteresis for short simulation times (Figure 6A, 10–20 ns, compare black with red symbols). Using $P_0 = 20\%$ does not yield a significant improvement for methanol compared to standard STeUS (Figure 6A, 10–20 ns, compare black with blue symbols). On the other hand, for the bulkier permeants, atenolol, 1-propranolol, and ibuprofen, using 50% occupancy at the ground temperature leads to poorer performance as compared to the standard STeUS with uniform occupancies (Figure 6B–D, black and red symbols). Conversely, increasing the occupancy of the ground temperature ($P_0 = 20\%$) leads to a small improvement in convergence, indicating that this might be suitable occupancy for bulkier permeants (Figure 6B–D, blue symbols).

DISCUSSION

We analyzed the convergence of PMF calculations for membrane permeation based either on conventional US simulations or on US augmented with simulated tempering (STeUS). Four solutes with different physicochemical characteristics were tested: methanol, atenolol, 1-propranolol, and ibuprofen (Table 1). Our analysis suggests that PMF calculations for bulky drug-like compounds converge poorly when using conventional US. The slow rearrangement of phospholipids is one factor generally contributing to the poor convergence of such simulations.^{2,5,31} For ibuprofen, sampling issues were furthermore found owing to slow rearrangements of the solute orientation or of intra-molecular dihedral angles.^{10,65} STeUS significantly improved sampling, greatly accelerating the convergence of the PMFs by at least fivefold (Figures 5 and 6). The improved convergence with STeUS was furthermore evident from the greatly reduced statistical error of the membrane partition coefficient for these solutes. In contrast, for small compounds such as methanol, conventional US performs well, suggesting that STeUS does not provide a benefit.

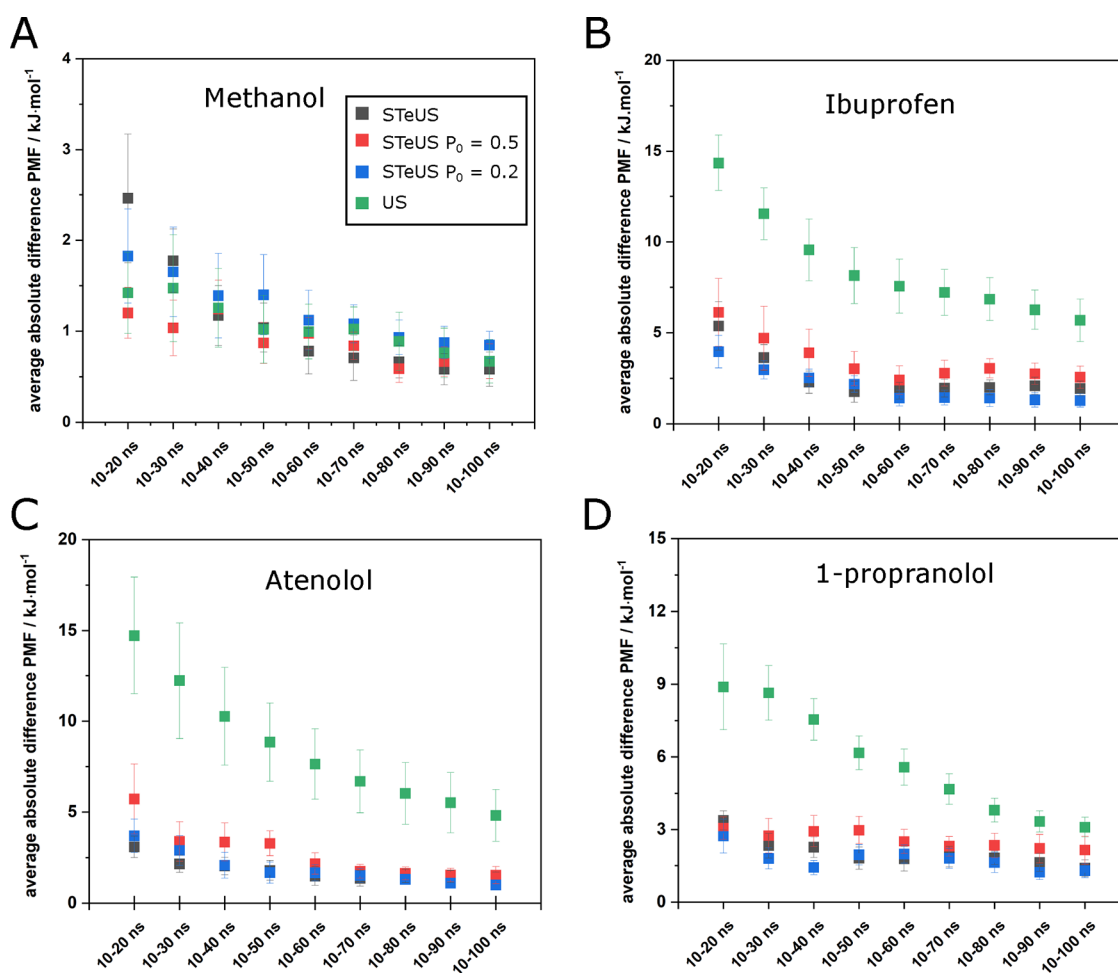


Figure 6. Average absolute difference between the PMFs for (A) methanol, (B) atenolol, (C) 1-propranolol, and (D) ibuprofen in the inward and outward directions, with increasing simulation times. The error in each point represents the standard error between the five independent replicas. Data points for each approach used (US, STeUS, and modified STeUS with $P_0 = 0.2$ and $P_0 = 0.5$) are depicted with different colors.

This study focused on sampling with the aim to obtain converged PMFs for a given force field, and we did not aim to refine the force fields against experimental data. For the interest of the reader, we note, however, that the computed water/membrane partition coefficients of the three bulkier molecules deviate significantly from experimental values (Table S1).

While potentially providing the benefit for overcoming enthalpic barriers, the conventional implementation of ST may lead to slower convergence of the umbrella histograms because only a fraction of $1/K$ of the simulation time is spent at the physiologically relevant ground temperature, where K is the number of temperature states (Figure 1). For larger simulation systems as compared to the membrane system simulated here, finer temperature steps and a larger K would be required, thereby further reducing the simulation time fraction spent at the ground temperature. To mitigate this limitation, we devised a modified ST implementation that allows the definition of the simulation time fraction P_0 spent at the ground temperature T_0 . Specifying P_0 enables finding a good balance between (i) simulating at T_0 to collect samples for the umbrella histograms and (ii) simulating at higher temperatures to overcome sampling barriers more rapidly. We found that an optimal choice of P_0 depends on the solute characteristics.

For the bulkier solutes, extensive sampling at higher temperatures was more critical and spending $P_0 = 11\%$ of

the simulation time at T_0 was sufficient for obtaining at least fivefold accelerated convergence. Increasing the occupancy of the ground temperature to $P_0 = 20\%$ further improved the convergence by a minor margin. For the small solute, methanol, for which the PMFs converged even with conventional US, STeUS achieved faster convergence only when spending $P_0 = 50\%$ at the ground temperature. Since (i) pharmaceutically relevant solutes are bulky, while (ii) PMF calculations with small solutes converge reasonably rapidly irrespective of the computational details, we suggest a value of $P_0 = 20\%$ as a useful starting point for future simulations.

The use of ST may lead to a moderate increase of computational cost as compared to US, because of the requirement of specific integrators. With GROMACS 2022, ST requires the use of the velocity Verlet integrator instead of the leap-frog integrator leading to a loss of computational efficiency of approximately 20% for the systems considered in this study. For the PMF calculations of bulkier compounds, this loss is by far outweighed by the convergence improvement, which is at least fivefold.

ST was previously used to enhance conventional MD simulations, for example, in the context of protein folding.^{66,67} To the best of our knowledge, this work for the first time combines ST with US and employs ST for studying solute permeation. An alternative to ST for membrane-solute permeation studies has been the use of replica exchange

methods.³⁷ Both replica exchange umbrella sampling (REUS)^{43,68} or umbrella sampling virtual replica exchange (US-VREX)⁶⁹ were previously demonstrated to improve PMF convergence as compared to conventional US. Similar to ST, replica-exchange methods may be used to conduct a walk along the temperature of the system, referred to as parallel tempering.³³ A disadvantage of replica exchange methods is the need for a larger number of inter-dependent parallel simulation replicas, which require the simultaneous allocation of a larger number of nodes on a compute cluster. In contrast, STeUS allows for a trivial parallelization with independent umbrella simulations, which enables the most efficient use of compute clusters. Furthermore, Rauscher et al.³⁷ suggested that ST-based methods are more efficient than replica exchange-based methods for sampling complex conformational landscapes. They also argued that, given that accurate weights are obtained, ST was the most efficient among the generalized-ensemble methods tested in their study.

CONCLUSIONS

We showed that the application of STeUS accelerates the convergence of PMFs (or free energy profiles) for membrane permeation of drug-like molecules as compared to the conventional US. The degree of improvement provided by STeUS was solute dependent. STeUS was particularly successful for bulky drug-like molecules, providing an at least fivefold increase of sampling efficiency. For smaller permeants, the application of simulated tempering was only beneficial if the system spends 50% of the simulation time at the physiologically relevant ground temperature. The option to define the proportion of time spent at the ground temperature was implemented in the modified ST protocol developed in this study. We expect STeUS to help in establishing all-atom MD simulations and PMF calculations as a routine method for predicting membrane permeabilities of large numbers of drug candidates.

ASSOCIATED CONTENT

Supporting Information

The Supporting Information is available free of charge at <https://pubs.acs.org/doi/10.1021/acs.jctc.2c01162>.

Supporting figures: temperature of the system along the simulation time, PMFs for each individual replica, boxplot representation of hysteresis for the US approach, PMFs with increasing simulation times for the STeUS approach, validation of the modified STeUS method, PMF of ibuprofen, as a function of solute distance from the bilayer COM, and absolute difference between the PMFs in the inward and outward directions of ibuprofen. Supporting tables: calculation of partition constants and comparison between US and STeUS (PDF)

Modified STeUS source code file for GROMACS 2021 (ZIP)

AUTHOR INFORMATION

Corresponding Author

Jochen S. Hub – *Theoretical Physics and Center for Biophysics (ZBP), Saarland University, 66123 Saarbrücken, Germany*; orcid.org/0000-0001-7716-1767; Email: jochen.hub@uni-saarland.de

Authors

Carla F. Sousa – *Drug Bioinformatics Group and Department of Biological Barriers and Drug Delivery, Helmholtz Institute for Pharmaceutical Research Saarland (HIPS), Helmholtz Centre for Infection Research (HZI), 66123 Saarbrücken, Germany*; orcid.org/0000-0002-6735-3455

Robert A. Becker – *Theoretical Physics and Center for Biophysics (ZBP), Saarland University, 66123 Saarbrücken, Germany*

Claus-Michael Lehr – *Department of Biological Barriers and Drug Delivery, Helmholtz Institute for Pharmaceutical Research Saarland (HIPS), Helmholtz Centre for Infection Research (HZI), 66123 Saarbrücken, Germany*; *Department of Pharmacy, Saarland University, 66123 Saarbrücken, Germany*

Olga V. Kalinina – *Drug Bioinformatics Group, Helmholtz Institute for Pharmaceutical Research Saarland (HIPS), Helmholtz Centre for Infection Research (HZI), 66123 Saarbrücken, Germany*; *Center for Bioinformatics, Saarland University, 66123 Saarbrücken, Germany*; *Medical Faculty, Saarland University, 66421 Homburg, Germany*

Complete contact information is available at: <https://pubs.acs.org/10.1021/acs.jctc.2c01162>

Author Contributions

The manuscript was written through contributions of all authors. All authors have given approval to the final version of the manuscript.

Notes

The authors declare no competing financial interest.

ACKNOWLEDGMENTS

C.F.S. gratefully acknowledges financial support by the “Singh-Chhatwal-Postdoctoral Fellowship Program,” of the “Friends of HZI” association. O.V.K. acknowledges the funding by the Klaus Faber Foundation. R.A.B. and J.S.H. were supported by the Deutsche Forschungsgemeinschaft (DFG, German Research Foundation, grant no. SFB 860/A16).

ABBREVIATIONS

US, umbrella sampling; ST, simulated tempering; STeUS, simulated tempering-enhanced umbrella sampling; MD, molecular dynamics; PMF, potential of mean force; T, temperature; WHAM, weighted histogram analysis method; POPC, palmitoyl-oleoyl-phosphatidylcholine; COM, center of mass

REFERENCES

- (1) Dror, R. O.; Dirks, R. M.; Grossman, J. P.; Xu, H.; Shaw, D. E. Biomolecular simulation: a computational microscope for molecular biology. *Annu. Rev. Biophys.* **2012**, *41*, 429–452.
- (2) Neale, C.; Bennett, W. F. D.; Tieleman, D. P.; Pomès, R. Statistical Convergence of Equilibrium Properties in Simulations of Molecular Solutes Embedded in Lipid Bilayers. *J. Chem. Theory Comput.* **2011**, *7*, 4175–4188.
- (3) Licari, G.; Dehghani-Ghahnaviyeh, S.; Tajkhorshid, E. Membrane Mixer: A Toolkit for Efficient Shuffling of Lipids in Heterogeneous Biological Membranes. *J. Chem. Inf. Model.* **2022**, *62*, 986–996.
- (4) Venable, R. M.; Krämer, A.; Pastor, R. W. Molecular Dynamics Simulations of Membrane Permeability. *Chem. Rev.* **2019**, *119*, 5954–5997.

- (5) Cardenas, A. E.; Elber, R. Computational study of peptide permeation through membrane: searching for hidden slow variables. *Mol. Phys.* **2013**, *111*, 3565–3578.
- (6) Sugano, K.; Kansy, M.; Artursson, P.; Avdeef, A.; Bendels, S.; Di, L.; Ecker, G. F.; Faller, B.; Fischer, H.; Gerebtzoff, G.; Lennernaes, H.; Senner, F. Coexistence of passive and carrier-mediated processes in drug transport. *Nat. Rev. Drug Discovery* **2010**, *9*, 597–614.
- (7) Ropponen, H.-K.; Richter, R.; Hirsch, A. K. H.; Lehr, C.-M. Mastering the Gram-negative bacterial barrier – Chemical approaches to increase bacterial bioavailability of antibiotics. *Adv. Drug Delivery Rev.* **2021**, *172*, 339–360.
- (8) Marrink, S.-J.; Berendsen, H. J. C. Simulation of water transport through a lipid membrane. *J. Phys. Chem.* **1994**, *98*, 4155–4168.
- (9) Awoonor-Williams, E.; Rowley, C. N. Molecular simulation of nonfacilitated membrane permeation. *Biochim. Biophys. Acta, Bio-membr.* **2016**, *1858*, 1672–1687.
- (10) Jämbeck, J. P. M.; Lyubartsev, A. P. Exploring the free energy landscape of solutes embedded in lipid bilayers. *J. Phys. Chem. Lett.* **2013**, *4*, 1781–1787.
- (11) Diamond, J. M.; Katz, Y. Interpretation of nonelectrolyte partition coefficients between dimyristoyl lecithin and water. *J. Membr. Biol.* **1974**, *17*, 121–154.
- (12) Orsi, M.; Essex, J. W. Permeability of drugs and hormones through a lipid bilayer: insights from dual-resolution molecular dynamics. *Soft Matter* **2010**, *6*, 3797–3808.
- (13) Loverde, S. M. Molecular Simulation of the Transport of Drugs across Model Membranes. *J. Phys. Chem. Lett.* **2014**, *5*, 1659–1665.
- (14) Lee, C. T.; Comer, J.; Herndon, C.; Leung, N.; Pavlova, A.; Swift, R. V.; Tung, C.; Rowley, C. N.; Amaro, R. E.; Chipot, C.; Wang, Y.; Gumbart, J. C. Simulation-Based Approaches for Determining Membrane Permeability of Small Compounds. *J. Chem. Inf. Model.* **2016**, *56*, 721–733.
- (15) Krämer, A.; Ghysels, A.; Wang, E.; Venable, R. M.; Klauda, J. B.; Brooks, B. R.; Pastor, R. W. Membrane permeability of small molecules from unbiased molecular dynamics simulations. *J. Chem. Phys.* **2020**, *153*, 124107.
- (16) Lei, H.; Duan, Y. Improved sampling methods for molecular simulation. *Curr. Opin. Struct. Biol.* **2007**, *17*, 187–191.
- (17) Lee, B. L.; Kuczera, K. Simulating the free energy of passive membrane permeation for small molecules. *Mol. Simul.* **2018**, *44*, 1147–1157.
- (18) Ghysels, A.; Roet, S.; Davoudi, S.; van Erp, T. S. Exact non-Markovian permeability from rare event simulations. *Phys. Rev. Res.* **2021**, *3*, No. 033068.
- (19) Comer, J.; Gumbart, J. C.; Hénin, J.; Lelièvre, T.; Pohorille, A.; Chipot, C. The Adaptive Biasing Force Method: Everything You Always Wanted To Know but Were Afraid To Ask. *J. Phys. Chem. B* **2015**, *119*, 1129–1151.
- (20) Bochicchio, D.; Panizon, E.; Ferrando, R.; Monticelli, L.; Rossi, G. Calculating the free energy of transfer of small solutes into a model lipid membrane: Comparison between metadynamics and umbrella sampling. *J. Chem. Phys.* **2015**, *143*, 144108.
- (21) Sun, R.; Dama, J. F.; Tan, J. S.; Rose, J. P.; Voth, G. A. Transition-Tempered Metadynamics Is a Promising Tool for Studying the Permeation of Drug-like Molecules through Membranes. *J. Chem. Theory Comput.* **2016**, *12*, 5157–5169.
- (22) Torrie, G. M.; Valleau, J. P. Nonphysical sampling distributions in Monte Carlo free-energy estimation: Umbrella sampling. *J. Comput. Phys.* **1977**, *23*, 187–199.
- (23) Zocher, F.; van der Spoel, D.; Pohl, P.; Hub, J. S. Local partition coefficients govern solute permeability of cholesterol-containing membranes. *Biophys. J.* **2013**, *105*, 2760–2770.
- (24) Wennberg, C. L.; van der Spoel, D.; Hub, J. S. Large Influence of Cholesterol on Solute Partitioning into Lipid Membranes. *J. Am. Chem. Soc.* **2012**, *134*, 5351–5361.
- (25) Sousa, C. F.; Coimbra, J. T. S.; Ferreira, M.; Pereira-Leite, C.; Reis, S.; Ramos, M. J.; Fernandes, P. A.; Gameiro, P. Passive Diffusion of Ciprofloxacin and its Metalloantibiotic: A Computational and Experimental study. *J. Mol. Biol.* **2021**, *433*, No. 166911.
- (26) Sousa, C. F.; Kamal, M. A. M.; Richter, R.; Elamaldeniya, K.; Hartmann, R. W.; Empting, M.; Lehr, C.-M.; Kalinina, O. V. Modeling the Effect of Hydrophobicity on the Passive Permeation of Solutes across a Bacterial Model Membrane. *J. Chem. Inf. Model.* **2022**, *62*, 5023–5033.
- (27) Kumar, S.; Rosenberg, J. M.; Bouzida, D.; Swendsen, R. H.; Kollman, P. A. THE weighted histogram analysis method for free-energy calculations on biomolecules. I. The method. *J. Comput. Chem.* **1992**, *13*, 1011–1021.
- (28) Stelzl, L. S.; Kells, A.; Rosta, E.; Hummer, G. Dynamic Histogram Analysis To Determine Free Energies and Rates from Biased Simulations. *J. Chem. Theory Comput.* **2017**, *13*, 6328–6342.
- (29) MacCallum, J. L.; Tieleman, D. P., Chapter 8 Interactions between Small Molecules and Lipid Bilayers. In *Current Topics in Membranes*, Feller, S. E., Ed. Academic Press: 2008; Vol. 60, pp. 227–256.
- (30) Bennion, B. J.; Be, N. A.; McNerney, M. W.; Lao, V.; Carlson, E. M.; Valdez, C. A.; Malfatti, M. A.; Enright, H. A.; Nguyen, T. H.; Lightstone, F. C.; Carpenter, T. S. Predicting a Drug's Membrane Permeability: A Computational Model Validated With in Vitro Permeability Assay Data. *J. Phys. Chem. B* **2017**, *121*, 5228–5237.
- (31) Neale, C.; Hsu, J. C.; Yip, C. M.; Pomès, R. Indolicidin binding induces thinning of a lipid bilayer. *Biophys. J.* **2014**, *106*, L29–L31.
- (32) Nitschke, N.; Atkovska, K.; Hub, J. S. Accelerating potential of mean force calculations for lipid membrane permeation: System size, reaction coordinate, solute-solute distance, and cutoffs. *J. Chem. Phys.* **2016**, *145*, 125101.
- (33) Hansmann, U. H. E. Parallel tempering algorithm for conformational studies of biological molecules. *Chem. Phys. Lett.* **1997**, *281*, 140–150.
- (34) Sugita, Y.; Okamoto, Y. Replica-exchange molecular dynamics method for protein folding. *Chem. Phys. Lett.* **1999**, *314*, 141–151.
- (35) Iba, Y. Extended Ensemble Monte Carlo. *Int. J. Mod. Phys. C* **2001**, *12*, 623–656.
- (36) Fukunishi, H.; Watanabe, O.; Takada, S. On the Hamiltonian replica exchange method for efficient sampling of biomolecular systems: Application to protein structure prediction. *J. Chem. Phys.* **2002**, *116*, 9058–9067.
- (37) Rauscher, S.; Neale, C.; Pomès, R. Simulated Tempering Distributed Replica Sampling, Virtual Replica Exchange, and Other Generalized-Ensemble Methods for Conformational Sampling. *J. Chem. Theory Comput.* **2009**, *5*, 2640–2662.
- (38) Hénin, J.; Lelièvre, T.; Shirts, M. R.; Valsson, O.; Delemotte, L. Enhanced sampling methods for molecular dynamics simulations. *arXiv* **2022**.
- (39) Marinari, E.; Parisi, G. Simulated Tempering: A New Monte Carlo Scheme. *EPL* **1992**, *19*, 451–458.
- (40) Geyer, C. J.; Thompson, E. A. Annealing Markov Chain Monte Carlo with Applications to Ancestral Inference. *J. Am. Stat. Assoc.* **1995**, *90*, 909–920.
- (41) Bussi, G.; Gervasio, F. L.; Laio, A.; Parrinello, M. Free-Energy Landscape for β Hairpin Folding from Combined Parallel Tempering and Metadynamics. *J. Am. Chem. Soc.* **2006**, *128*, 13435–13441.
- (42) Wang, L.; Friesner, R. A.; Berne, B. J. Replica Exchange with Solute Scaling: A More Efficient Version of Replica Exchange with Solute Tempering (REST2). *J. Phys. Chem. B* **2011**, *115*, 9431–9438.
- (43) Sugita, Y.; Kitao, A.; Okamoto, Y. Multidimensional replica-exchange method for free-energy calculations. *J. Chem. Phys.* **2000**, *113*, 6042–6051.
- (44) Piana, S.; Laio, A. A Bias-Exchange Approach to Protein Folding. *J. Phys. Chem. B* **2007**, *111*, 4553–4559.
- (45) Sugita, Y.; Mitsutake, A.; Okamoto, Y., Generalized-ensemble algorithms for protein folding simulations. In *Rugged Free Energy Landscapes*, Springer: 2008; pp. 369–407.
- (46) Metropolis, N.; Rosenbluth, A. W.; Rosenbluth, M. N.; Teller, A. H.; Teller, E. Equation of State Calculations by Fast Computing Machines. *J. Chem. Phys.* **1953**, *21*, 1087–1092.
- (47) Park, S.; Pande, V. S. Choosing weights for simulated tempering. *Phys. Rev. E* **2007**, *76*, No. 016703.

- (48) Wang, F.; Landau, D. P. Efficient, Multiple-Range Random Walk Algorithm to Calculate the Density of States. *Phys. Rev. Lett.* **2001**, *86*, 2050–2053.
- (49) Li, Y.; Protopopescu, V. A.; Gorin, A. Accelerated simulated tempering. *Phys. Lett. A* **2004**, *328*, 274–283.
- (50) Berger, O.; Edholm, O.; Jähnig, F. Molecular dynamics simulations of a fluid bilayer of dipalmitoylphosphatidylcholine at full hydration, constant pressure, and constant temperature. *Biophys. J.* **1997**, *72*, 2002–2013.
- (51) Tieleman, D. P.; Berendsen, H. J. A molecular dynamics study of the pores formed by Escherichia coli OmpF porin in a fully hydrated palmitoyloleoylphosphatidylcholine bilayer. *Biophys. J.* **1998**, *74*, 2786–2801.
- (52) Berendsen, H. J. C.; Postma, J. P. M.; van Gunsteren, W. F.; Hermans, J., Interaction Models for Water in Relation to Protein Hydration. In *Intermolecular Forces: Proceedings of the Fourteenth Jerusalem Symposium on Quantum Chemistry and Biochemistry Held in Jerusalem, Israel, April 13–16, 1981*, Pullman, B., Ed. Springer Netherlands: Dordrecht, 1981; pp. 331–342.
- (53) Malde, A. K.; Zuo, L.; Breeze, M.; Stroet, M.; Poger, D.; Nair, P. C.; Oostenbrink, C.; Mark, A. E. An Automated Force Field Topology Builder (ATB) and Repository: Version 1.0. *J. Chem. Theory Comput.* **2011**, *7*, 4026–4037.
- (54) Berendsen, H. J. C.; van der Spoel, D.; van Drunen, R. GROMACS: A message-passing parallel molecular dynamics implementation. *Comput. Phys. Commun.* **1995**, *91*, 43–56.
- (55) Van Der Spoel, D.; Lindahl, E.; Hess, B.; Groenhof, G.; Mark, A. E.; Berendsen, H. J. C. GROMACS: Fast, flexible, and free. *J. Comput. Chem.* **2005**, *26*, 1701–1718.
- (56) Humphrey, W.; Dalke, A.; Schulten, K. VMD: Visual molecular dynamics. *J. Mol. Graphics* **1996**, *14*, 33–38.
- (57) Darden, T.; York, D.; Pedersen, L. Particle mesh Ewald: An N-log(N) method for Ewald sums in large systems. *J. Chem. Phys.* **1993**, *98*, 10089–10092.
- (58) Essmann, U.; Perera, L.; Berkowitz, M. L.; Darden, T.; Lee, H.; Pedersen, L. G. A smooth particle mesh Ewald method. *J. Chem. Phys.* **1995**, *103*, 8577–8593.
- (59) Allen, M. P.; Tildesley, D. J. *Computer Simulations of Liquids*. Oxford University Press: Oxford, U. K., 1984; p 64–65.
- (60) Bussi, G.; Donadio, D.; Parrinello, M. Canonical sampling through velocity rescaling. *J. Chem. Phys.* **2007**, *126*, No. 014101.
- (61) Berendsen, H. J. C.; Postma, J. P. M.; van Gunsteren, W. F.; DiNola, A.; Haak, J. R. Molecular dynamics with coupling to an external bath. *J. Chem. Phys.* **1984**, *81*, 3684–3690.
- (62) Hess, B.; Bekker, H.; Berendsen, H. J. C.; Fraaije, J. G. E. M. LINCS: A linear constraint solver for molecular simulations. *J. Comput. Chem.* **1997**, *18*, 1463–1472.
- (63) Miyamoto, S.; Kollman, P. A. Settle: An analytical version of the SHAKE and RATTLE algorithm for rigid water models. *J. Comput. Chem.* **1992**, *13*, 952–962.
- (64) Hub, J. S.; de Groot, B. L.; van der Spoel, D. g_wham—A Free Weighted Histogram Analysis Implementation Including Robust Error and Autocorrelation Estimates. *J. Chem. Theory Comput.* **2010**, *6*, 3713–3720.
- (65) Badaoui, M.; Kells, A.; Molteni, C.; Dickson, C. J.; Hornak, V.; Rosta, E. Calculating Kinetic Rates and Membrane Permeability from Biased Simulations. *J. Phys. Chem. B* **2018**, *122*, 11571–11578.
- (66) Hansmann, U. H. E.; Okamoto, Y. Numerical comparisons of three recently proposed algorithms in the protein folding problem. *J. Comput. Chem.* **1997**, *18*, 920–933.
- (67) Irbäck, A.; Pothast, F. Studies of an off-lattice model for protein folding: Sequence dependence and improved sampling at finite temperature. *J. Chem. Phys.* **1995**, *103*, 10298–10305.
- (68) Pokhrel, N.; Maibaum, L. Free Energy Calculations of Membrane Permeation: Challenges Due to Strong Headgroup–Solute Interactions. *J. Chem. Theory Comput.* **2018**, *14*, 1762–1771.
- (69) Neale, C.; Madill, C.; Rauscher, S.; Pomès, R. Accelerating Convergence in Molecular Dynamics Simulations of Solutes in Lipid

Membranes by Conducting a Random Walk along the Bilayer Normal. *J. Chem. Theory Comput.* **2013**, *9*, 3686–3703.

Recommended by ACS

Phosphorylation Regulation Mechanism of $\beta 2$ Integrin for the Binding of Filamin Revealed by Markov State Model

Xiaokun Hong, Hai-Feng Chen, *et al.*

JANUARY 06, 2023
JOURNAL OF CHEMICAL INFORMATION AND MODELING

READ 

Exploring the Transferability of Replica Exchange Structure Reservoirs to Accelerate Generation of Ensembles for Alternate Hamiltonians or Protein Mutations

Koushik Kasavajhala and Carlos Simmerling

MARCH 02, 2023
JOURNAL OF CHEMICAL THEORY AND COMPUTATION

READ 

Optimal Bond Constraint Topology for Molecular Dynamics Simulations of Cholesterol

Balázs Fábíán, Gerhard Hummer, *et al.*

FEBRUARY 17, 2023
JOURNAL OF CHEMICAL THEORY AND COMPUTATION

READ 

Stochastic Approximation to MBAR and TRAM: Batchwise Free Energy Estimation

Maaïke M. Galama, Frank Noé, *et al.*

JANUARY 23, 2023
JOURNAL OF CHEMICAL THEORY AND COMPUTATION

READ 

Get More Suggestions >